GEOPHYSICAL RESEARCH LETTERS, VOL. 24, NO. 23, PAGES 2981-2984, DECEMBER 1, 1997

Topographically generated gravity waves in the Brooks Range, Alaska

Amanda H. Lynch

Cooperative Institute for Research in Environmental Sciences, University of Colorado, Boulder, Colorado

Abstract. Amplified wind events are identified over the Brooks Range in Alaska, with observed wind speed increasing from calm to 5 ms^{-1} over 24 to 36 hours. In simulations using an limited area climate system model, the wind events are captured consistently, although generally display greater strength than observed. Cooling associated with the wind events lead to an identification of the NE region of the North Slope of Alaska, below the inversion, as the source region for the air flow. Analysis of the wind event of 7th January 1992 supports the nonlinear hydraulic model of gravity waves.

Introduction

Strong downslope surface winds are often observed along the lee slopes of mountain ranges in the midlatitudes, and are generally so ubiquitous that they have local names: the Alpine foehn, the Rocky Mountain chinook, and the Argentine zonda, for example. Every few years, the eastern slope of the Rocky Mountains experiences a windstorm so severe that maximum gusts as high as 60 ms^{-1} are observed. Observational studies have suggested that favorable conditions for downslope winds are upstream wind speeds of 7-15 ms^{-1} within 30° perpendicular to the ridgeline, and an upstream layer of strong stability near mountaintop level (Colson 1954, Brinkmann 1974). In the relative calm of continental winter climate in northern Alaska, such strong wind gusts are rarely observed, and downslope windstorms in the Brooks Range of northern Alaska are not generally well known. However, ample anecdotal evidence exists to suggest that such windstorms do occur in this region (L. Hinzman, pers. comm.), and while their strength does not rival a Rocky Mountain chinook, they are significant for several reasons. In a region where aviation is a primary means of transport, the pervasiveness of powdery snow makes visibility sensitive to even weak wind events. In addition, the temperatures are already so low in this region that modest winds can lead to dangerous wind chill factors.

Effects of a Mountain Barrier: The Linear Model

When a stably stratified airstream flows over a topographic barrier, vertically propagating gravity waves are excited, transferring energy and momentum away from the barrier. In the presence of such waves, the pressure is systematically higher on the upwind slopes than on the leeward ones (Bannon and Yuhas 1990), and a net force is exerted on the ground. The most important wavelengths associated with this momentum transport are of the order of tens of kilometres (Bretherton 1969, McFarlane 1987). Simulation of these waves in a global climate model (GCM) is difficult since they are sub-grid-scale events in such models. In addition, the smoothing of orography in GCMs distorts terrain shape as well as scale, which has a significant impact upon the influence of the topography on the impinging flow (Pierrehumbert 1984).

In GCM applications, this problem has been addessed by using an orographic enhancement such as "envelope" or "silhouette" orography (e.g. Wallace et al. 1983), or by introducing a parameterization which includes the effects of the momentum transport by the gravity waves using (generally) a linear approximation. However, in addition to their impact on the momentum balance of the general circulation, and on the stratospheric pole to equator temperature gradient, these wave motions play a role in the development of strong downslope wind events such as those studied by Durran (1986). Such wind events should be resolved and detectable in a model of sufficient grid resolution.

Many of the basic features of observed mountain waves can be represented using simple linear theory for a steady monochromatic wave (McFarlane 1987). If we consider that we can represent the incident flow as a strongly stable lower layer topped by a weakly stable upper layer, a two layer model using the shallow water equations can represent the flow (Holton 1982). The perturbation solution to such a system is:

$$h' = -\frac{h_M(\bar{u}^2/c^2)}{(1-\bar{u}^2/c^2)} \qquad u' = \frac{h_M}{H}\left(\frac{\bar{u}}{1-\bar{u}^2/c^2}\right) \tag{1}$$

where h' is the deviation of the top of the lower layer, u' is the acceleration of the mean flow $\bar{u}$, c is the wave speed, h_M is the height of the mountain and H is the total depth of the layers. The shallow water wave speed is

$$c^2 = gH\delta\rho/\rho_1 \tag{2}$$

where ρ_1 is the mean density over the lower layer and $\delta\rho$ the deviation in the density. The characteristics of the flow can be described by the magnitude of the Froude number

$$Fr \equiv \bar{u}^2/c^2 \tag{3}$$

When $Fr<1$, the flow is subcritical, the wave speed is greater than the mean flow speed, and $h'<0$. When $Fr>1$, the flow is supercritical, and the wave speed is less than the mean flow speed. Thus, the waves are swept downstream from the ridge and cannot play a role in establishing a steady state adjustment between the height and velocity disturbances. When $Fr\sim1$, the disturbances are no longer small and the linear solution breaks down.

Since data documenting these waves in the Brooks Range of northern Alaska is extrememly limited, a regional climate model experiment was performed to determine whether mountain waves could be simulated. Section 2 describes the model and the experiment, and section 3 focusses on a particular case which occurs in January 1992.

Paper number 97GL03017.
0094-8534/97/97GL-03017$05.00

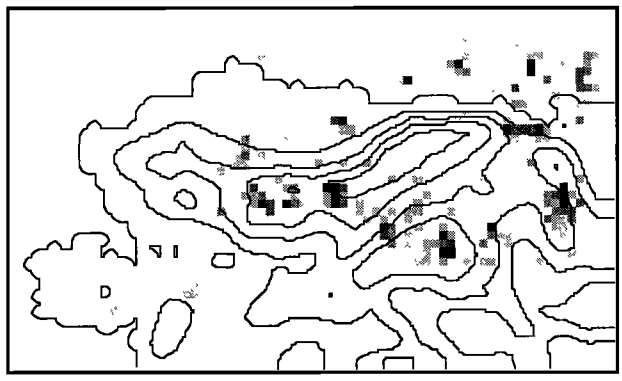

Figure 1. Location of simulated low pressure systems during the month of January 1992 superimposed onto topography contours (300 m contour interval) and Alaskan coastline (solid lines). Darker colors indicate more systems found at that grid point throughout the month. Systems are indicated at every grid point they pass through during the life of the system.

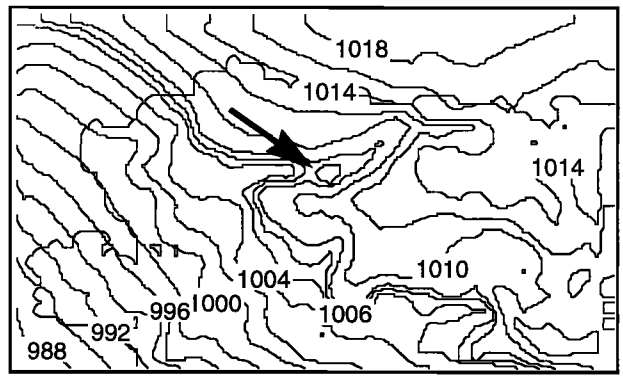

Figure 2. Simulated mean sea level pressure contours on 7th January 1992, at which time the low pressure center (indicated by an arrow) has a central pressure of 1006 hPa with a Laplacian of 2.84.

Model Experiment

The Arctic Region Climate System Model (ARCSyM) is a coupled atmosphere-land-sea ice-ocean model consisting of a hydrostatic, primitive-equation atmospheric model based upon the NCAR Regional Climate Model Version 2 (RegCM2; Giorgi et al. 1993); the Biosphere-Atmosphere Transfer Scheme (BATS1E) land surface/vegetation model (Dickinson et al 1993); a dynamic sea ice model incorporating the Flato and Hibler (1992) cavitating fluid rheology with a modified shear stress formulation, and Parkinson and Washington (1979) 2-layer ice thermodynamics; and several ocean model formulations (1 dimensional mixed layer, 3 dimensional primitive equation ocean circulation model). Details of the model formulation can be found in Lynch et al. (1995). The ARCSyM model is initialized and forced at the lateral boundaries by observational analyses from the European Centre for Medium-Range Weather Forecasting (ECMWF) for the year 1992. Note that the ECMWF analyses rely on sparse data in this region (5 upper air stations in the region of interest), but they are the best available. The computational domain is the North Slope of Alaska (Figure 1), and consists of a horizontal grid at 20 km resolution, with 23 vertical levels in the atmosphere (highest resolution in the boundary layer). In this case, the sea ice and ocean are specified rather than explicitly modeled. The ocean model is replaced by a "swamp ocean" which consists of a constant heat flux and specified sea surface temperatures (Shea et al. 1992). The sea ice concentration is specified using observations derived from SSM/I data. The sea ice thickness and surface fluxes are calculated using the sea ice thermodynamics component, but no ice dynamical motion is allowed, and sea ice thickness is forced to remain consistent with the specified concentration. The simulation described here is examined in detail in Lynch et al. (1997).

Focus on January 1992

An efficient means of gauging the pressure variations in the model simulation is to count the number of cyclones which occur, and plot their locations. This was done using an algorithm developed by Serreze et al. (1997) which accounts for cyclogenesis, movement and cyclolysis of low pressure systems exceeding a minimum strength. The criterion for a low pressure system was a pressure difference over 40 km of at least 2 hPa, and the systems were tracked from one six hourly period to the next. Since the algorithm detects pressure deficits rather than cyclonic circulation, it also reveals any regions of consistent low pressure which would indicate mountain wave drag. The procedure was performed for all months in the annual cycle simulation. In addition, the same field was filtered and rebalanced to a 200 km horizontal grid spacing. This was done to ascertain the effects of resolution, and to distinguish between the large scale forcing and the smaller scale effects of mountain waves. It was found that cyclonic developments at the 200 km scale correspond well with the large scale pressure fields from the ECMWF analyses, indicating the dominance of lateral forcing at this scale. Figure 1 shows the locations of low pressure regions found using this procedure (without the filtering) for the model simulated mean sea level pressure field for January 1992. There are several preferential sites for low pressure regions to develop - in particular, the southern and western leeward edges of the Brooks Range were highly favorable locations for an atmospheric pressure deficit, and this area will be the focus of this paper.

As an illustration of the low pressure regions detected on the mesoscale, consider the low pressure region which is diagnosed on the 6th January and is maintained until the 10th. Figure 2 shows the mean sea level pressure field on the 7th January, and indicates the low pressure region on the southwestern lee edge of the Brooks Range. The area covered by detectably low pressure is

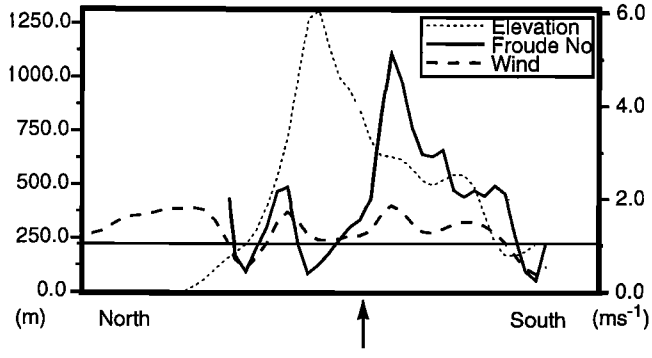

Figure 3. Lowest model level Froude number (bold solid) over the topography (dotted) and component of the wind speed (bold dashed) along a cross-section from the Beaufort sea to the Yukon River Valley. The Fr=1 level is indicated by a solid line, and the location of the low pressure center is indicated by an arrow. The wind acceleration can be seen clearly just to the south.

less than 150 km across, and hence falls well inside the average resolution of a global climate model or the observational analyses. In the prevailing north to north-easterly flow during this period, the linear theory predicts that the low pressure region indicates the presence of vertically propagating gravity waves. However, although partial reflection of these vertically propagating linear gravity waves may produce enhanced surface winds under some conditions (Klemp and Lilly 1975), in general nonlinear processes are essential to account for observed windstorms associated with stable flow over topography (Richard et al. 1989, Durran 1990). Since in this case, a strongly stable lower layer topped by a weakly stable upper layer is observed in the model simulation (not shown), the shallow water equations can still be used. In the nonlinear form, the governing equation is

$$(1 - Fr^2)\frac{\partial u}{\partial x} = \frac{ug}{c^2}\frac{\partial h_M}{\partial x} \tag{4}$$

where c is the wave speed, h_M is the height of the mountain and H is the total depth of the layers. The shallow water wave speed in this case is

$$c^2 = g(h - h_M) \tag{5}$$

and the conditions for subcritical and supercritical flow are the same as in the linear theory. From equation (4), the flow will accelerate on the upslope side of the ridge if $Fr<1$ but will decelerate if $Fr>1$, and vice versa on the downslope side of the ridge. Fr can also be understood in this case to be proportional to the ratio of the magnitude of nonlinear advection to the magnitude in the changes in pressure gradient generated by changes in the fluid depth (Durran 1990). Thus, in supercritical flow, the nonlinear advection term dominates and balance is satisfied only when the flow is accelerated. This behavior can be seen to some degree in Figure 3, which shows a cross section across the Brooks Range of the topography, the wind speed and the Froude number. In this case, Fr does not reach unity at the crest, and hence flow remains subcritical and starts to decelerate on the lee side of the mountain. However, the flow does become supercritical partway down the slope and starts to accelerate strongly as it descends the lee side. Thus, the waves are swept downstream from the ridge and cannot play a role in establishing a steady state adjustment between the height and velocity disturbances. Hence the flow can only adjust back to the ambient subcritical conditions in a turbulent hydraulic jump, producing high velocities along the lee slope.

Figure 4 shows the passage of this wind event through a particular point over time. The model (Fig. 4(a)) shows that the wind

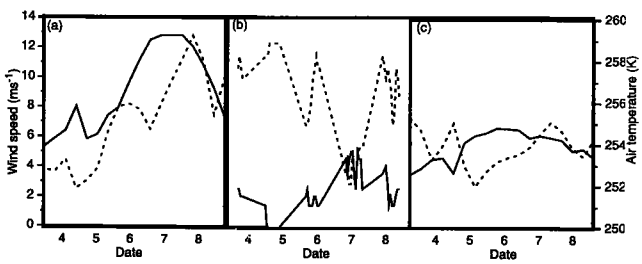

Figure 4. Time series of wind speed (solid) and air temperature (dashed) from (a) model simulation at simulated low pressure centre location on 7th January, at lowest model level (about 70m); (b) station data at Bettles, the closest station to low pressure centre, at anemometer level; and (c) model simulation at Bettles, at lowest model level (about 70m).

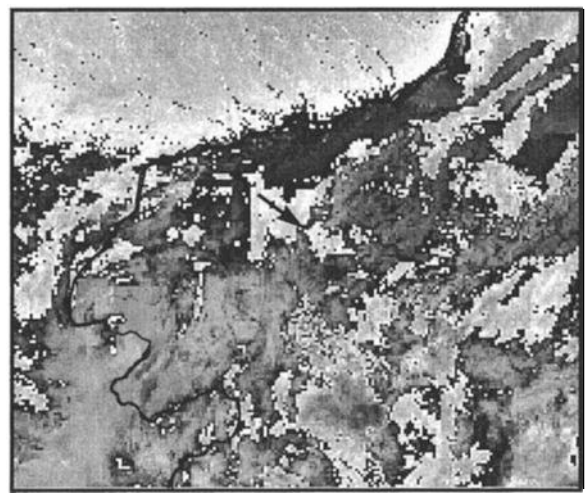

Figure 5. AVHRR image (false color) for 7th January 1992, showing the low pressure region location (black arrow).

speed at the lowest model level (about 60m) more than doubles from 6 ms^{-1} to 12 ms^{-1} over a period of two days. To confirm that this event was observed, the wind data at several nearby stations was examined. The anemometer level data at Bettles (just to the south of the low pressure location, Fig. 4(b)) shows a qualitatively similar acceleration in the wind speed, from near calm to 5 ms^{-1}, and the lowest model level simulation at this location (Fig. 4(c)) corresponds well with this behavior, although the higher altitude of the model, combined with the fact that Bettles in situated in a river valley, results in a response which is more gradual but with higher absolute wind speeds. Note that the calm period in the Bettles record is not missing data. AVHRR data (Advanced Very High Resolution Radiometer, Figure 5) shows a small amount of low level cloud over the low pressure location, indicating a limited area of vertical motion. Figure 4 also shows the temperature time series (dashed) for the lowest model level, and for the station data. The station data indicates that as the high winds pass through, the temperature drops dramatically by 6 K. A weaker drop of 3 K is seen for the lowest model level at the station location, and a smaller drop of only 1.5 K is simulated at the low pressure center. This is in contrast to typical midlatitude topographically induced gravity waves, in which strong adiabatic warming as the upper

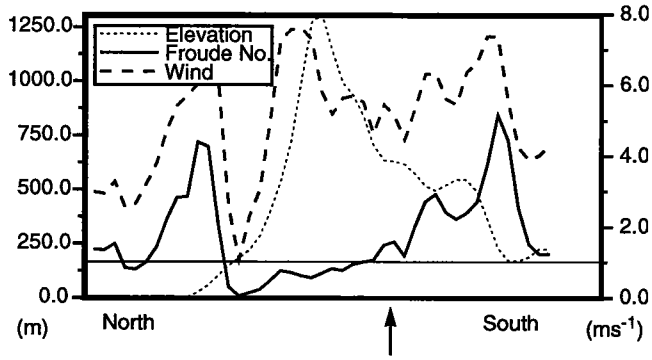

Figure 6. Lowest model level Froude number (bold solid) over the topography (dotted) and component of the wind speed (bold dashed) for 24th January 1992 along a cross-section from the Beaufort sea to the Yukon River Valley. The Fr=1 level is indicated by a solid line, and the location of the low pressure center is indicated by an arrow.

level air descends the leeward side of the range causes temperature rises to be observed in association with any downslope wind event (Richard et al. 1989). From an analysis of simulated wind fields and equivalent potential temperature (which is approximately conserved in this process, not shown), the source region for the air in the downslope wind event is lower tropospheric (around 850 hPa), below the inversion, and over the extremely cold northeast region of the North Slope of Alaska, where the atmospheric temperatures are well below 250 K. To illustrate the effects of these low temperatures, consider a saturated parcel of air from the source region lifted pseudo-adiabatically to complete condensation, and then returned adiabatically to its original pressure height. At 275 K, such a parcel would be warmed by approximately 12 K. In contrast, at 250 K, the warming would be, at most, 1 K. Thus, such flow in Arctic regions does not lead to the adiabatic warming observed in mid-latitude events, and in this case, a net cooling is in fact observed.

Several other events captured by the cyclonic activity algorithm were examined for consistency with the above case study. Figure 6 shows the Froude Number and wind speed associated with a low pressure center detected on 24th January 1992. While station data for this event was not available, the model simulation clearly exhibits the same behavior, and if anything, shows a clearer relationship to the non-linear hydraulic theory. With the $Fr<1$, the wind speed increases as it ascends the barrier, and decreases as it descends the leeward side, until the Froude Number exceeds unity, at which point the wind speed increases dramatically, and then adjusts rapidly back to the mean flow.

Summary

Amplified wind fields in the lee of the Brooks Range in northern Alaska are indicated in the station data; satellite data and simulations by the Arctic Regional Climate System Model are consistent with these observations. Non-dimensional analysis of the model fields shows good agreement with the hydraulic model of downslope windstorms. This study represents the first detailed analysis of such systems in Alaska; in a state strongly dependent on aviation, such events warrant further attention, and more detailed observation.

Acknowledgements. The author thanks D. McGinnis and M. Serreze for data analysis assistance and discussions early in the piece, and also N. McFarlane, who made some helpful comments. Special thanks are due J. Walsh for insightful observations, and extremely useful critiques of the manuscript. This work was supported by the NSF Arctic System Science Program through Grant OPP-9214810.

References

Bannon, P.R. and J.A.Yuhas, 1990: On mountain wave drag over complex terrain. *Meteorol. Atmos. Phys.*, **43**, 155-162.

Bretherton, F.P., 1969: Momentum transport by gravity waves *Quart. J. Roy. Met. Soc.*, **95**, 213-242.

Brinkmann, W.A.R , 1974: Strong downslope winds at Boulder, Colorado. *Mon.Wea.Rev.*, **102**, 592-602.

Colson, D., 1954: Meteorological problems in forecasting mountain waves *Bull. Amer. Meteor. Soc.*, **35**, 363-371.

Dickinson, R.E , A. Henderson-Sellers and P.J. Kennedy, 1993: Biosphere-Atmosphere Transfer Scheme (BATS) version 1E as coupled to the NCAR Community Climate Model. *NCAR Tech. Note* NCAR/TN-387+STR, 72pp.

Durran, D.R., 1986: Another look at downslope windstorms. Part I: On the development of analogs to supercritical flow in an infinitely deep, continuously stratified fluid. *J. Atmos. Sci.*, **43**, 2527-2543.

Durran, D.R., 1990: Mountain waves and downslope winds. In *Atmospheric Processes over Complex Terrain*, W. Blumen, ed., AMS, 59-81.

Flato, G.M., and W D. Hibler III, 1992: Modeling pack ice as a cavitating fluid. *J. Phys. Oceanogr.*, 22, 626-651.

Giorgi, F., M.R. Marinucci, and G.T. Bates, 1993: Development of a second generation regional climate model (RegCM2). Part I: Boundary-layer and radiative transfer processes. *Mon. Wea. Rev.*, 121, 2794-2813.

Holton, J.R., 1982: *An Introduction to Dynamic Meteorology, 3rd ed.* Academic Press, San Diego, CA, 511pp.

Klemp, J.B. and D.K. Lilly, 1975: The dynamics of wave induced downslope winds *J. Atmos Sci.*, **32**, 320-339.

Lynch, A.H., W.L. Chapman, J.E Walsh, and G. Weller, 1995: Development of a regional climate model of the western Arctic. *J. Climate*, **8**, 1555-1570.

Lynch, A.H., D.L. McGinnis, and D.A. Bailey, 1997: The seasonal cycle and snow melt in a regional climate system model: Influence of land surface model. *J. Geophy. Res.*, (in review).

McFarlane, N.A., 1987: The effect of orographically excited gravity wave drag on the general circulation of the lower stratosphere and troposphere. *J. Atmos. Sci.*, **44**, 1775-1800.

Parkinson, C. L. and W. M. Washington, 1979: A large-scale numerical model of sea ice, *J. Geophy. Res.*, 84(C1), 311-337.

Pierrehumbert, R.T., 1984: Linear results on the barrier effects of mesoscale mountains. *J.Atmos.Sci.*, **41**, 1356-1367.

Richard, E., P. Mascart and E.C. Nickerson, 1989: The role of surface friction in downslope windstorms. *J. Appl. Meteorol.*, **28**, 241-251.

Serreze, M.C , F. Carse, R.G. Barry amd J.C. Rogers, 1997: Icelandic Low cyclone activity: climatological features, linkages with the NAO, and relationships with recent changes in the Northern Hemisphere circulation, *J. Climate*, **10**, 453-464

Shea, D.J., K.E. Trenberth and R W. Reynolds, 1992: A global monthly sea surface temperature climatology. *J.Climate*, **5**, 987-1001.

Wallace, J., S. Tibaldi and A. Simmons, 1983: Reduction of systematic forecast errors in the ECMWF model through the introduction of an envelope orography. *Quart. J. Roy. Meteor. Soc.*, **109**, 683-717.

A. H. Lynch, Cooperative Institute for Research in Environmental Sciences, CB 216, University of Colorado, Boulder, CO 80309. (e-mail: manda@tok.colorado.edu)

(Received May 21, 1997; revised October 8, 1997;
accepted October 13, 1997)